Spreading area and shape regulate apoptosis and differentiation of osteoblasts

2013 Biomed. Mater. 8 055005

(http://iopscience.iop.org/1748-605X/8/5/055005)

Biomed. Mater. **8** (2013) 055005 (8pp) doi:10.1088/1748-6041/8/5/055005

Spreading area and shape regulate apoptosis and differentiation of osteoblasts

Ruirong Fu[1,5], **Qinli Liu**[1,2,5], **Guanbin Song**[2], **Andrew Baik**[3], **Man Hu**[1], **Shujin Sun**[1], **X Edward Guo**[3], **Mian Long**[1,6] **and Bo Huo**[1,4,6]

[1] Key Laboratory of Microgravity and Center for Biomechanics and Bioengineering, Institute of Mechanics, Chinese Academy of Sciences, Beijing 100190, People's Republic of China
[2] College of Bioengineering, Chongqing University, Chongqing 400030, People's Republic of China
[3] Department of Biomedical Engineering, Columbia University, New York, USA
[4] School of Aerospace Engineering, Beijing Institute of Technology, Beijing 100081, People's Republic of China

E-mail: huobo@bit.edu.cn and mlong@imech.ac.cn

Received 22 May 2013
Accepted for publication 14 August 2013
Published 3 September 2013
Online at stacks.iop.org/BMM/8/055005

Abstract

The *in vivo* observations have indicated that at the remodeling sites of bone, the spreading area or shape of preosteoblasts is confined by the mineralized matrix. But it remains unknown whether this spreading confinement regulates the differentiation or apoptosis of osteoblasts. In the present study, osteoblast-like cells (MC3T3-E1) were seeded on micropatterned islands with different area and shape. The expression of three osteogenic differentiation markers was measured by immunofluorescence staining and apoptotic cells were detected using a terminal deoxyribonucleotidyl transferase-mediated dUTP nick end labelling assay kit. The membrane fluorescence staining results showed that the actual spreading area of micropatterned osteoblasts coincided with the designed value. When the area of a micropatterned cell was confined as 314 or 615 μm^2, which was lower than that of freely spreading osteoblasts, the circular shape promoted the expression of osteogenic differentiation markers and the percentage of apoptotic osteoblasts compared with the branched shape. This shape-regulated differentiation and apoptosis of osteoblasts with confined spreading area were abolished when actin polymerization was inhibited by cytochalasin D. The present study gives an insight into the roles of spreading morphology on osteoblastic differentiation and apoptosis.

(Some figures may appear in colour only in the online journal)

Introduction

Osteoblasts are derived from bone marrow mesenchymal stem cells (MSCs) and eventually differentiate into osteocytes. At the remodeling sites, preosteoblasts on bone surface are activated and then produce a matrix of osteoid, which further becomes mineralized. The mineralized extracellular matrix stiffens and confines the spreading size (e.g. area) or shape (e.g. circularity or aspect ratio) of osteoblasts. A morphometric investigation showed that there was a 70% volume reduction in the mature osteocytes' cell body compared to the volume of original osteoblasts [1]. This means that the *in vivo* cell–matrix contact area of osteocytes decreases up to 45% of osteoblasts. In addition, it seems that the differentiation process is initiated by the rounding of the spindle- or triangle-shaped preosteoblasts followed by extending their protrusion into the minerals [2]. These osteoblasts are gradually embedded into the matrix and finally become dendritic osteocytes [2, 3]. Except for the spreading confinement-relating differentiation,

[5] The first two authors equally contributed to this work.
[6] Authors to whom any correspondence should be addressed.

it was believed that about 50% to 70% of those osteoblasts that were initially present at the remodeling site underwent apoptosis [4]. But it remains unknown whether and how the confined spreading size and shape regulate osteoblastic differentiation or apoptosis.

Certain cues for some cell lineages have revealed that cell differentiation is correlated with spreading size. Watt *et al* found that the rounded human epidermal keratinocytes on smaller islands (400 μm^2) were stimulated toward terminal differentiation [5]. This conclusion was reconfirmed that higher population of keratinocytes differentiated when they were cultured on small (20 μm diameter) circular islands than large (50 μm diameter) ones [6]. The similar tendency of rounded cell to differentiate was further demonstrated in hepatocytes [7], human mesenchymal stem cells (hMSCs) [8, 9]. For the pluripotent stem cells, cell size decides their fate. For example, hMSCs allowed to fully spread (10 000 μm^2) on a substrate underwent smooth muscle cell differentiation, but those hMSCs prevented from spreading and flattening (1024 μm^2) were found to have upregulated chondrogenic genes [10]. When cells are cultured on the patterns with same area, cell shape plays a key role in regulating the differentiation of unipotent or pluripotent stem cells. The smaller aspect ratio, i.e. the higher circularity, enhanced the terminal differentiation of hepatocyte [7] and keratinocytes [6]. For MSCs, the circular shape-induced adipogenesis [11–14] and those shapes with smaller circularity, e.g. larger aspect ratio rectangle or star-like one, promote osteogenesis [13, 14].

It has been extensively studied that cell size regulates cell growth. For example, as the reduction of cell area often accompanies with the increase of cell height, the growth of these rounded endothelial cells is significantly inhibited [15, 16]. Another earlier study showed that DNA synthesis decreased in hepatocytes on relatively smaller adhesive island (1600 μm^2) [7]. In addition, smaller islands or beads (100 μm^2) made more endothelial cells to enter into apoptosis, whereas the cells on larger islands (4000 μm^2) grew normally [17, 18]. The abovementioned cell size-dependent cell growth was recently observed in other cell lines such as fibroblasts, osteoblasts, and MSCs [19]. To our knowledge, however, there has not been a direct investigation on the relation between cell shape and cell death or growth excluding the effect of cell size.

In the present study, the micropatterning technique was adopted to control the spreading shape and area of mouse (MC3T3-E1) osteoblast-like cells, then the osteogenesis and the apoptosis were detected before and after the inhibition of F-actin formation. The results indicated that the osteoblasts confined in the smaller patterns tended to differentiate or to undergo apoptosis, while a wrinkled shape (lower circularity) reduced this small size-induced differentiation or apoptosis. It was further demonstrated that the F-actin synthesis regulated this size- or shape-dependent phenomenon.

Materials and methods

Surface fabrication

Four types of patterns were designed: a circle and circles with short, medium, or long rectangular branches, which have

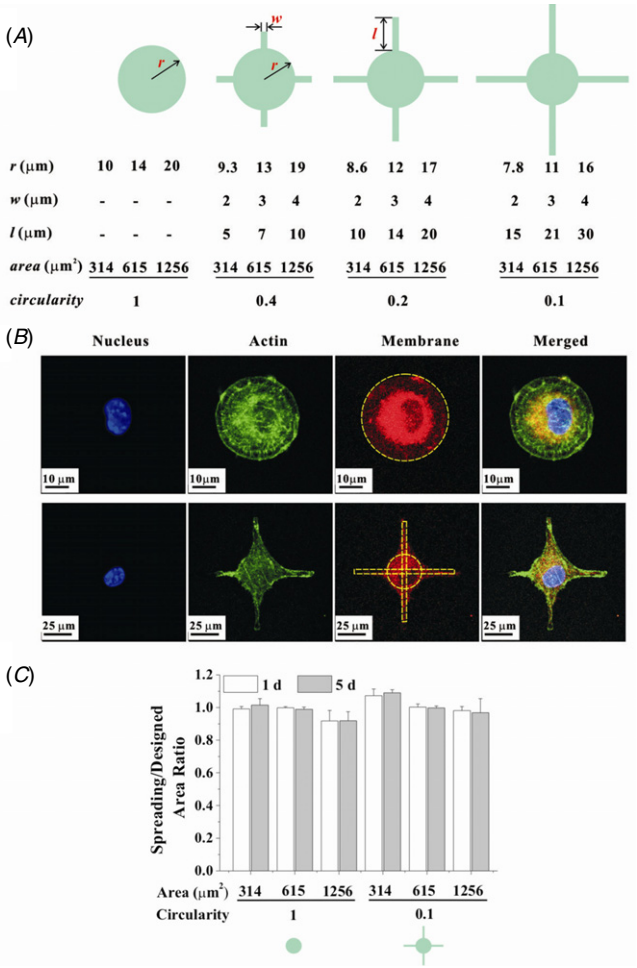

Figure 1. Spreading shapes and areas of cells. (*A*) Designed patterns and corresponding geometric parameters: radius *r* of the circle, length *l* and width *w* of a branch, area, and circularity. (*B*) Fluorescent images of the nucleus, actin, and membrane of MC3T3-E1 cells cultured on two 1256 μm^2 patterns: circle (upper row) and circle with a long branch (lower row). In the membrane staining images, the *yellow dashed line* indicates the designed contour of the pattern. The right column shows the merged images of the nucleus, actin, and membrane. (*C*) Ratio of the actual spreading area of cells at 1 and 5 days after seeding to the designed area of patterns with different shapes and areas.

decreasing circularities of 1.0, 0.4, 0.2, and 0.1, respectively (figure 1(*A*)). For one type of patterns, the circularities were kept constant by adjusting the circle radii and the branch lengths. Three areas of 314, 615, and 1256 μm^2 were chosen so that the diameters of the corresponding circles are 20, 28, 40 μm, respectively. The typical spreading area of MC3T3-E1 cells on unpatterned surface is about 1200 μm^2. Other two areas were adopted to mimic the spreading-confined condition. These designed patterns were replicated on a polydimethylsiloxane stamp as introduced in our previous papers [20–22]. The hydrophilization of the stamp was achieved by sputtering oxygen ions on the stamp's surface with a SBC-12 ion sputter coater (KYKY Technology Company, Beijing). A comb-polymer (purchased from Suzhou Nanotechnology Institute, CAS) was used to obtain the micropatterned substrate, which remained stable for approximately three months [23]. Briefly, one droplet of the

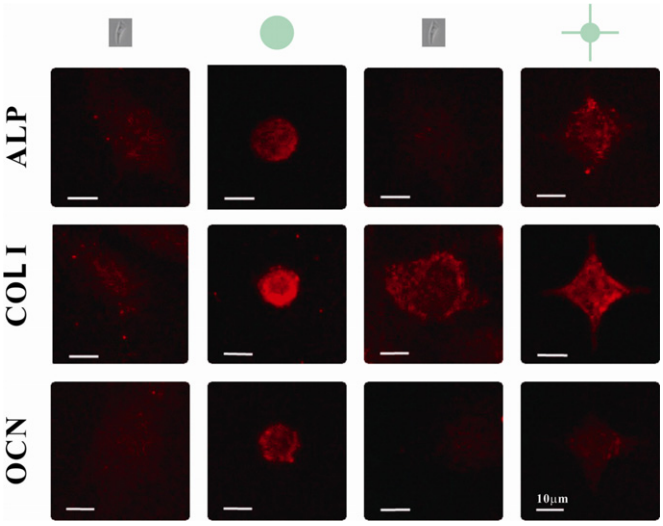

Figure 2. Fluorescent images showing the rhodamine-labeled protein expression of ALP, COL I, and OCN of cells cultured on the micropatterned regions (second and fourth columns) and those cultured on regions without patterns in the same slide (corresponding left columns). Images were collected at 1 day after seeding.

comb-polymer solution was placed on the stamp surface and was made uniform by centrifugation at 1500 rpm. Then, the stamp was gently pressed onto a culture dish for 10 s before the designed patterns were transferred onto the surface of a culture dish.

Cell culture

Mouse MC3T3-E1 osteoblast-like cells (Subclone 4, ATCC, USA) within passage numbers 13 were cultured in an α-minimum essential medium (Hyclone, USA) supplemented with 10% fetal bovine serum (Gibco, USA) plus 1% penicillin and streptomycin (Hyclone, USA) at 37 °C in a humidified atmosphere of 95% air and 5% CO_2. In this study we didn't utilize the differentiation medium such as ascorbic acid that is recommended by ATCC as positive control because the differentiation capacity of MC3T3-E1 had been demonstrated by a previous study [24]. The cells were seeded on micropatterned culture dishes at a density of 3×10^3 cells cm^{-2} such that they attached to the regions that were not stamped with the comb-polymer. After seeding for 1 h, the culture dish was gently washed to remove unattached cells. In the group for disrupting cytoskeleton, the seeded cells were cultured in a medium with 1 μg mL^{-1} cytochalasin D (CD, Sigma-Aldrich Co.) for 24 h to inhibit actin polymerization.

Identification of cellular spreading area and shape

To identify whether cells spread complying with the designed geometry, a membrane fluorescent dye Vybrant CM-DiI (Molecular Probes, Inc., USA) was used to visualize the cell contour. Phalloidin (Alexis Biochemicals, USA) and Hoechst stain (Invitrogen, USA) were employed to display actin structure and nuclear position, respectively. First, the slides with micropatterned cells were incubated with 0.5% CM-DiI in α-minimum essential medium at 37 °C for 15 min. Then, the cells were fixed with 4% paraformaldehyde at room temperature for 15 min and permeabilized with 0.4% Triton-X-100 in phosphate-buffered saline (PBS) at room temperature for 15 min. After rinsing with PBS, the cells were stained with a 2% fluorescein isothiocyanate (FITC)-phalloidin working solution (Boster Company, Wuhan, P R China) by incubation at room temperature for 60 min. The cells were subsequently counterstained with Hoechst stain by incubation at room temperature for 15 min. Finally, the cells were observed under a LSM 510 META confocal system (Carl Zeiss, Jena, Germany). The spreading contour of a cell was manually drawn from the CM-DiI staining photo and then was used to calculate the spreading area of this cell.

Differentiation measurements

After the cells were grown on a micropatterned surface for either 1 or 5 days, they were gently washed with PBS, fixed with 4% paraformaldehyde in PBS for 15 min at room temperature, and permeabilized with 0.4% Triton-X-100 in PBS for 15 min at room temperature. Then, the cells were incubated with goat anti-mouse polyclonal antibodies against alkaline phosphatase (ALP), type I collagen (COL I), or osteocalcin (OCN; Santa Cruz Biotechnology, Inc., USA) at a 1:100 dilution for 60 min at 37 °C, which was followed by three washes with PBS and a subsequent incubation in the dark for 60 min with either a rhodamine-labeled affinity-purified antibody to goat IgG (KPL, Inc., USA) at a 1:100 dilution or to phalloidin (Alexis Biochemicals, USA) at a 1:200 dilution. The cell nuclei were additionally counterstained with 0.1% Hoechst stain in PBS in the dark for 60 min. Finally, the cells were visualized using a fluorescence microscope (IX-71; Olympus).

Apoptosis assay

A terminal deoxyribonucleotidyl transferase-mediated dUTP-digoxigenin nick end labeling (TUNEL) assay kit (In Situ Cell Death Detection Kit; Roche) was used to detect the apoptosis of micropatterned osteoblasts. After fixation, the cells were blocked with 0.3% hydrogen peroxide in methanol for 10 min at room temperature and permeabilized with 0.1% Triton-X-100 in sodium citrate for 2 min on ice. Then, the cells were incubated with a TUNEL reaction mixture of the label solution and the enzyme solution for 60 min at 37 °C in a humidified atmosphere in the dark, which was followed by rinses with PBS and a subsequent incubation with the peroxidase-conjugated Converter-POD solution for 30 min at 37 °C. The slides were then incubated with the DAB (3,3-diaminobenzidine-tetrahydrochloride) substrate (Boster Company, Wuhan, P R China) for 10 min. Finally, a hematoxylin counterstain was used to stain the nuclear regions. When observed under a light microscope, the cells in apoptosis revealed brownish yellow particles at nuclear regions (figure 4(*A*)). About ten fields in one sample were chosen, and at least three samples were collected for each case.

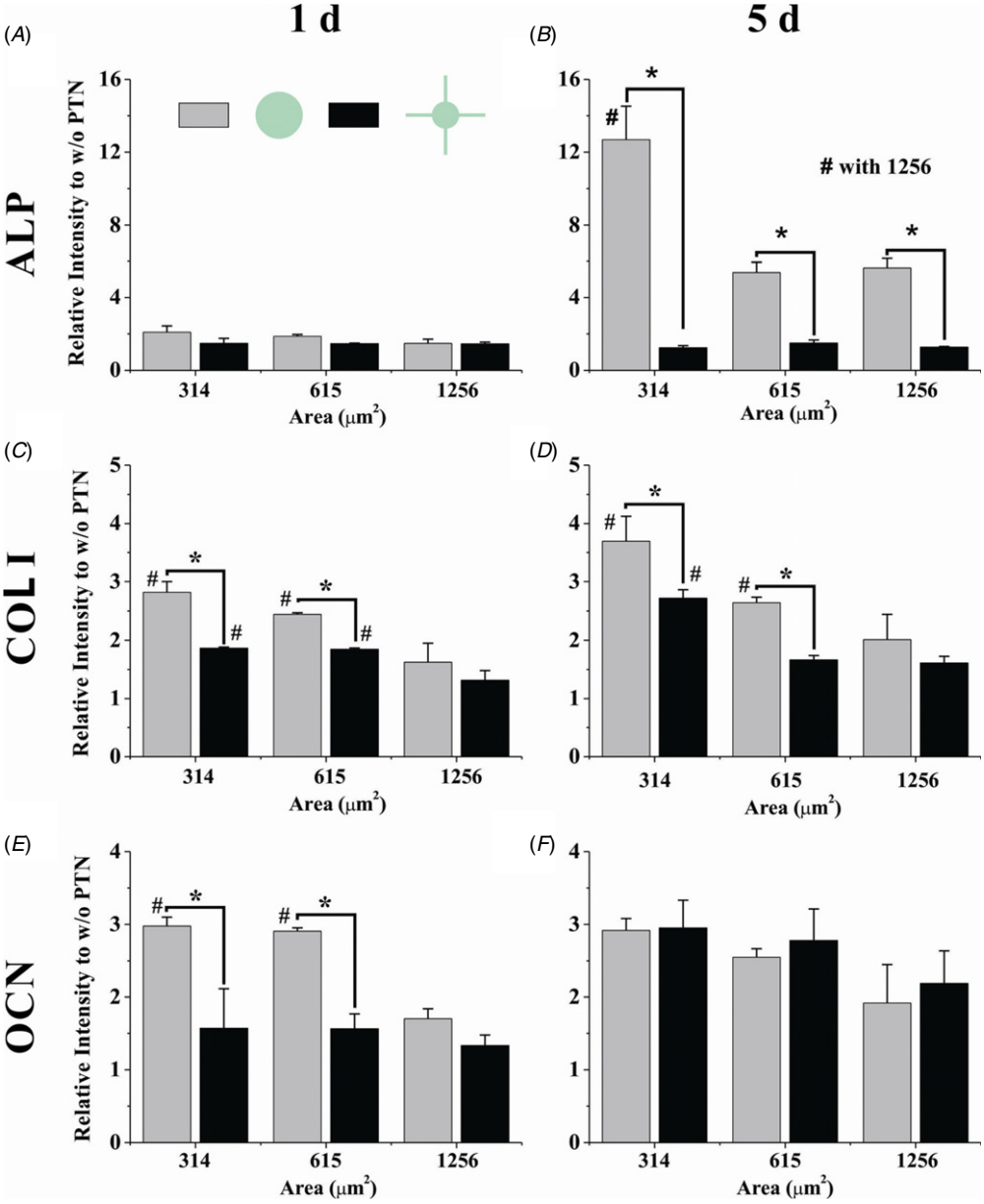

Figure 3. Relative fluorescent intensity of differentiation markers of MC3T3-E1 cells at 1 and 5 days after seeding (mean ± SE). * and # represent a significant difference ($p < 0.05$).

Data analysis and statistics

In this study, data were collected only from those cells spreading as one cell in one micropatterned island. For the analysis of cell differentiation, the relative fluorescent intensity of a differentiation marker in one slide was calculated using the following equation:

$$\frac{1}{n_p}\sum_i \left(f^i_{pc} - f^i_{pb}\right) \Big/ \frac{1}{n_r}\sum_i \left(f^i_{rc} - f^i_{rb}\right),$$

where f^i_{pc} is the mean fluorescent intensity of the ith micropatterned cell body, f^i_{pb} that of a neighboring background region around the ith micropatterned cell, f^i_{rc} and f^i_{rb} those of the cells cultured on the regions without comb-polymer patterns in the same slide, and n_p and n_r are the numbers of counted cells on the micropatterned and randomly cultured regions, respectively.

All experiments were performed at least in triplicate, and at least 30 cells were measured for each replicate. The data were analyzed using the software ImageJ (version 1.42q for Microsoft Windows; National Institutes of Health, USA) and presented as mean ± SD if not specifically claimed. One-way analysis of variance (ANOVA) with Bonferroni's post hoc analysis was performed to determine the statistically significant differences between the mean values of different groups ($p < 0.05$).

Results

Cells spread consistently with designed patterns

When cells were seeded on the micropatterned surfaces, they attached and spread on the adhesive islands. The cellular

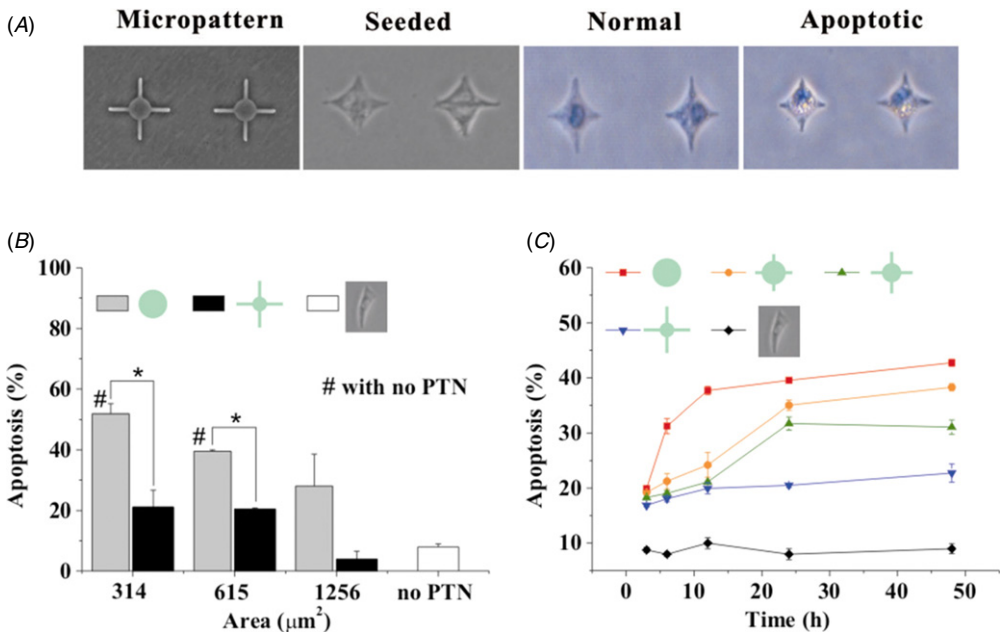

Figure 4. Effect of cell shapes and areas on the apoptosis of MC3T3-E1 cells. (*A*) Light microscopic images of the micropatterned surface with a comb-polymer, seeded cells, and TUNEL-labeled cells in normal and apoptotic states. (*B*) Apoptosis percentage of cells on patterns of different shapes and areas at 1 day after seeding (mean ± SE). (*C*) Variation of apoptosis percentage of cells on 314 μm^2 patterns with different shapes at different times after seeding (mean ± SE). PTN, pattern. * and # represent a significant difference ($p < 0.05$).

spreading shapes were consistent with the designed patterns, as typically shown in figure 1(*B*). Furthermore, the ratios of actual/designed spreading areas were nearly one and no significant differences were detected for different designed areas, shapes, and seeding durations (figure 1(*C*)).

Circularity regulated osteogenic differentiation

Figure 2 showed fluorescent images of the rhodamine-labeled osteogenic differentiation markers, namely, ALP, COL I, and OCN. Figure 3 presented the relative fluorescent intensity of three osteogenic differentiation markers of ALP, COL I, and OCN. At 1 day after seeding, the osteoblasts cultured on circular islands expressed significantly higher levels of COL I and OCN than those with long branches (figures 3(*C*) and (*E*)). In addition, they had higher levels on smaller islands such as 314 and 615 μm^2 than 1256 μm^2 islands. Although there was no significant difference for the ALP expression among different cell shapes and areas at 1 day after seeding (figure 3(*A*)), the cells with a circular pattern expressed a much higher ALP level at 5 days after seeding (figure 3(*B*)) Moreover, the ALP levels on the branched pattern did not change compared with those cells at 1 day after seeding. The COL I at 5 days after seeding maintained a similar shape-dependence as those at 1 day after seeding but their expression levels had completely increased (figure 3(*D*)). The cell shape-induced difference of OCN that was observed in 1-day-seeding osteoblasts disappeared in 5-day-seeding group, mainly due to the increase of OCN levels on patterns with long branches (figure 3(*F*)). Therefore, the shapes and sizes of osteoblasts cooperatively regulate their osteogenic differentiation.

Circularity determined cellular survival

Apoptotic cells that were labeled positively by TUNEL assay were counted (figure 4(*A*)). When cells were cultured for 1 day, about 50% of the cells on 314 μm^2 circular patterns underwent apoptosis, as shown in figure 4(*B*). However, only 20% of cells had died on the patterns with a smaller circularity of 0.1. For a specific area, the apoptosis percentages between circularities 1 and 0.1 were significantly different. With an increased cell area, more cells survived. When the cell area increased to a normal spreading value of 1256 μm^2, the cell status on patterns with long branches was similar to the cells cultured on unpatterned regions. In the case of 314 μm^2 pattern, cell death was about 20% independent of cell shape at the initial 3 h after seeding (figure 4(*C*)). Along with the increase in the circularities and seeding time, more cells entered into apoptosis. For example, cells on patterns with circularities of 0.1, 0.2, 0.4, and 1 caused an apoptosis percentage of 23%, 31%, 38%, and 43%, respectively, at 48 h after seeding. In addition, the apoptosis percentage of cells with the smallest circularity of 0.1 did not change obviously with different seeding times. Meanwhile, the apoptosis percentage of randomly cultured cells was kept constant as low as about 8%. The above results showed that cell shape but not cell size is crucial in regulating cell apoptosis.

Disruption of F-actin inhibited shape-induced apoptosis and differentiation

In this study, CD was used to inhibit the polymerization of actin monomers in order to investigate the relationship between cytoskeleton and osteoblastic survival and differentiation. It was shown that after CD treatment, the spreading area

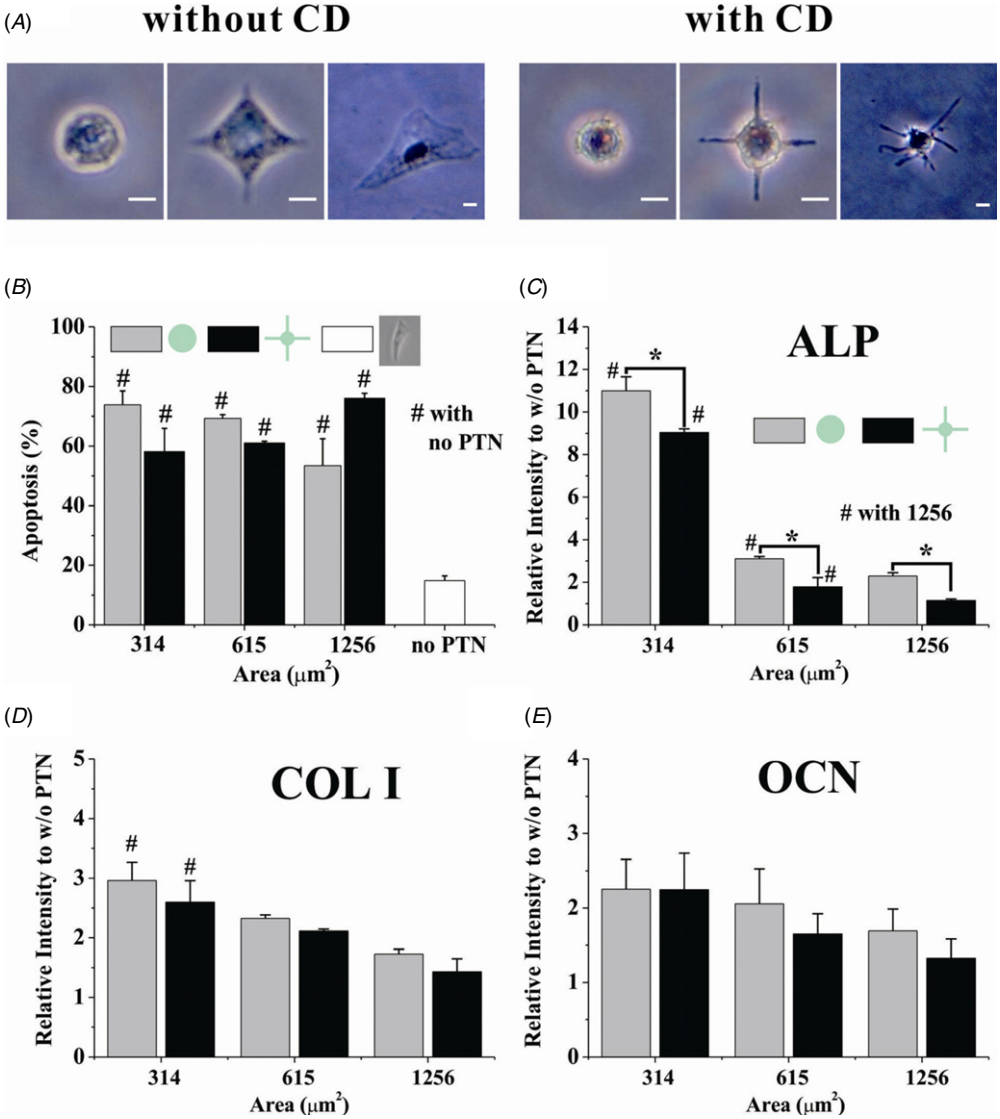

Figure 5. The effect of disrupting F-actin by cytochalasin D on cell apoptosis and differentiation. Light microscopic images (*A*), apoptosis percentage (*B*) and expression of differentiation markers (*C*)–(*E*) of osteoblasts after incubation with cytochalasin D for 24 h (mean ± SE). The spreading area of cells in (*A*) is 314 μm^2 and the scale bar is 10 μm. PTN, pattern. * and # represent a significant difference ($p < 0.05$).

of micropatterned or unpatterned cells obviously shrank, which occurred more dramatically for the cell protrusions (figure 5(*A*)). The apoptosis percentage of 1-day-seeding osteoblasts grown on branched patterns reached 58% to 76%, which is a comparable level to that on circular patterns (figure 5(*B*)), indicating that the branched shape doesn't maintain cell viability when the actin fibers are disrupted. The cells cultured on blank regions without patterns kept a relatively low apoptotic percentage of 15%. The shape-dependent expression of COL I and OCN also disappeared after F-actin was disrupted (figures 5(*D*) and (*E*)). By contrast, the expression level of ALP in cells on circular patterns was still higher than branched patterns (figure 5(*C*)), while its level had evidently increased as compared with cells grown on similar conditions but without CD. These results suggested that the shape-dependent apoptosis and differentiation of the cells are strongly related to actin polymerization.

Discussion

The present study demonstrated that both spreading shape and size of osteoblasts regulated cell differentiation and apoptosis. It is suggested that osteoblasts with bigger circularity expressed more differentiation markers and had a high level of apoptosis, while the branched osteoblasts grew normally and tended to keep their original cell lineage. One supporting *in vivo* observation for this conclusion is that osteoblasts initially become rounded during the differentiation process before they are embedded in the mineral matrix to become dendritic osteocytes [2]. Our present study provides direct evidence that even in a smaller spreading area, the cells with branched shape can retain their original state but those with circular shape cannot.

Three osteogenic marker proteins of ALP, COL I, and OCN were detected in this study and their expression levels revealed a cell shape-dependent tendency. However, the

shape-induced differences were not observed in the ALP expression at 1 day and the OCN expression at 5 days after seeding. It should be noted that for the cells with circular pattern at 5-day seeding, ALP expression level increased greatly, while COL I expression only increased slightly but OCN expression level didn't significantly changed. A previous study has demonstrated that when MC3T3-E1 cells were exposed to ascorbic acid, the mRNA levels of COL I, ALP and OCN remarkably increased at 24, 48 and 96 h, respectively [25]. When MC3T3-E1 cells were induced to differentiate by statin, the mRNA levels of ALP, COL I and OCN significantly increased at longer time, i.e. 7, 8 and 12 days [26]. The latter study showed a timeline of three differentiation markers similar to our results, i.e. ALP expression was earlier than COL I that was followed by OCN. In addition, the present data also indicated that the expression levels of COL I and OCN on the branched surface are similar to those on the circular surface at a normal spreading area of 1256 μm^2, thereby implying that branched pattern leads to a similar lineage commitment for osteoblasts compared with unpatterned surface. The signaling pathways of shape-induced are being investigated in our lab.

One straightforward interpretation of the shape-dependent cell apoptosis and differentiation is that cytoskeleton remodeling plays a key role in both processes. The shape of micropatterned islands probably controls the focal adhesion assembly [27, 28], influences the formation of F-actin [29], changes the structure of the cytoskeleton-related proteins [30, 31], and finally influences the cell nuclei to modify gene expression as well as other cellular behaviors [32, 33]. One previous study indicated that short-term CD treatment increased ALP activity, OCN secretion and mineralization of the extracellular matrix in MC3T3-E1 cells, with temporary changes in actin cytoskeleton [34]. Our current study demonstrated that breaking up the actin network with CD significantly reduced the shape-dependent cell apoptosis and differentiation. However, the capacity of cell shape to influence the distribution of adhesion complex, change cytoskeleton structure, and regulate cellular behavior, as well as the mechanisms involved, are still unknown. Related studies are in progress in our laboratory.

Acknowledgments

This work was supported by the National Natural Science Foundation of China (30970707) (BH), the National Key Basic Research Foundation of China (2011CB710904), and the National Natural Science Foundation of China (31110103918) (ML).

References

[1] Palumbo C 1986 A three-dimensional ultrastructural study of osteoid-osteocytes in the tibia of chick embryos *Cell Tissue Res.* **246** 125–31

[2] Knothe Tate M L *et al* 2004 The osteocyte *Int. J. Biochem. Cell Biol.* **36** 1–8

[3] van Hove R P *et al* 2009 Osteocyte morphology in human tibiae of different bone pathologies with different bone mineral density—is there a role for mechanosensing? *Bone* **45** 321–9

[4] Jilka R L *et al* 1998 Osteoblast programmed cell death (apoptosis): modulation by growth factors and cytokines *J. Bone Miner. Res.* **13** 793–802

[5] Watt F M, Jordan P W and O'Neill C H 1988 Cell shape controls terminal differentiation of human epidermal keratinocytes *Proc. Natl Acad. Sci. USA* **85** 5576–80

[6] Connelly J T *et al* 2010 Actin and serum response factor transduce physical cues from the microenvironment to regulate epidermal stem cell fate decisions *Nature Cell Biol.* **12** 711–8

[7] Singhvi R *et al* 1994 Engineering cell shape and function *Science* **264** 696–8

[8] McBeath R *et al* 2004 Cell shape, cytoskeletal tension, and RhoA regulate stem cell lineage commitment *Dev. Cell* **6** 483–95

[9] Song W, Kawazoe N and Chen G P 2011 Dependence of spreading and differentiation of mesenchymal stem cells on micropatterned surface area *J. Nanomater.* **2011** 1–9

[10] Gao L, McBeath R and Chen C S 2010 Stem cell shape regulates a chondrogenic versus myogenic fate through Rac1 and N-cadherin *Stem Cells* **28** 564–72

[11] Song W *et al* 2011 Adipogenic differentiation of individual mesenchymal stem cell on different geometric micropatterns *Langmuir* **27** 6155–62

[12] Wang X *et al* 2013 Influence of cell protrusion and spreading on adipogenic differentiation of mesenchymal stem cells on micropatterned surfaces *Soft Matter* **9** 4160–6

[13] Kilian K A *et al* 2010 Geometric cues for directing the differentiation of mesenchymal stem cells *Proc. Natl Acad. Sci. USA* **107** 4872–7

[14] Peng R, Yao X and Ding J 2011 Effect of cell anisotropy on differentiation of stem cells on micropatterned surfaces through the controlled single cell adhesion *Biomaterials* **32** 8048–57

[15] Folkman J and Moscona A 1978 Role of cell shape in growth control *Nature* **273** 345–9

[16] Ingber D E 1990 Fibronectin controls capillary endothelial cell growth by modulating cell shape *Proc. Natl Acad. Sci. USA* **87** 3579–83

[17] Chen C S *et al* 1997 Geometric control of cell life and death *Science* **276** 1425–8

[18] Chen C S *et al* 1998 Micropatterned surfaces for control of cell shape, position, and function *Biotechnol. Prog.* **14** 356–63

[19] Yan C, Sun J and Ding J 2011 Critical areas of cell adhesion on micropatterned surfaces *Biomaterials* **32** 3931–8

[20] Huo B *et al* 2010 An ATP-dependent mechanism mediates intercellular calcium signaling in bone cell network under single cell nanoindentation *Cell Calcium* **47** 234–41

[21] Huo B *et al* 2008 Fluid flow induced calcium response in bone cell network *Cell Mol. Bioeng.* **1** 58–66

[22] Lu X L *et al* 2012 Osteocytic network is more responsive in calcium signaling than osteoblastic network under fluid flow *J. Bone Miner. Res.* **27** 563–74

[23] Ma H W *et al* 2005 Fabrication of biofunctionalized quasi-three-dimensional microstructures of a nonfouling comb polymer using soft lithography *Adv. Funct. Mater.* **15** 529–40

[24] Wang D *et al* 1999 Isolation and characterization of MC3T3-E1 preosteoblast subclones with distinct *in vitro* and *in vivo* differentiation/mineralization potential *J. Bone Miner. Res.* **14** 893–903

[25] Franceschi R T and Iyer B S 1992 Relationship between collagen synthesis and expression of the osteoblast phenotype in MC3T3-E1 cells *J. Bone Miner. Res.* **7** 235–46

[26] Maeda T *et al* 2004 Induction of osteoblast differentiation indices by statins in MC3T3-E1 cells *J. Cell. Biochem.* **92** 458–71

[27] Chen C S *et al* 2003 Cell shape provides global control of focal adhesion assembly *Biochem. Biophys. Res. Commun.* **307** 355–61
[28] Lavenus S *et al* 2011 Behaviour of mesenchymal stem cells, fibroblasts and osteoblasts on smooth surfaces *Acta Biomater.* **7** 1525–34
[29] Pollard T D and Cooper J A 2009 Actin, a central player in cell shape and movement *Science* **326** 1208–12
[30] Mendez M G, Kojima S I and Goldman R D 2010 Vimentin induces changes in cell shape, motility, and adhesion during the epithelial to mesenchymal transition *FASEB J.* **24** 1838–51
[31] Damania D *et al* 2010 Role of cytoskeleton in controlling the disorder strength of cellular nanoscale architecture *Biophys. J.* **99** 989–96
[32] Rudolf E *et al* 2005 Hexavalent chromium disrupts the actin cytoskeleton and induces mitochondria-dependent apoptosis in human dermal fibroblasts *Toxicol. In Vitro.* **19** 713–23
[33] Vetterkind S *et al* 2005 Binding of Par-4 to the actin cytoskeleton is essential for Par-4/Dlk-mediated apoptosis *Exp. Cell Res.* **305** 392–408
[34] Higuchi C *et al* 2009 Transient dynamic actin cytoskeletal change stimulates the osteoblastic differentiation *J. Bone Miner. Metab.* **27** 158–67